RSC Advances

COMMUNICATION

View Article Online
View Journal | View Issue

Cite this: *RSC Adv.*, 2015, **5**, 17104

Received 18th December 2014
Accepted 3rd February 2015

DOI: 10.1039/c4ra16635c

www.rsc.org/advances

Effect of Zn and Zr addition on the synthesis of an $AlH_3/MgCl_2$ nanocomposite and its de-hydriding properties†

Duan Congwen, Hu Lianxi* and Sun Yu

This paper presents the preliminary findings of the effects of 3d transition metals on the synthesis of an $AlH_3/MgCl_2$ nanocomposite and its de-hydriding properties. The average grain size of as-milled AlH_3 is 4–6 nm with a desirable hydrogen desorption content of 9.69 wt%, indicating that AlH_3 is a promising hydrogen-storage material.

Because of efficient power generation and zero greenhouse gas emission, hydrogen storage has proved to be one of the most considerable interests for researchers.[1–5] However, there are many technical barriers in its implementation, such as the lack of lightweight, high-density, low-cost hydrogen storage materials.[6,7] Over the recent decades, many solid media including complex chemical and metal–organic hydrides have been explored as promising hydrogen storage candidates,[8–10] among which aluminum hydride (AlH_3) is a desirable metastable binary hydride and crystalline solid at room temperature. It has a hydrogen content of 10.1 wt% and a volumetric hydrogen density of 148 g H_2 per L.[11,12] AlH_3–etherate was initially synthesized by Finholt in 1947,[13] but the experimental results did not attract significant attention (see eqn (1)). Brower successfully synthesized non-solvated AlH_3 from $LiAlH_4$ and $AlCl_3$ in diethyl ether in 1976,[14] demonstrating that AlH_3 has at least six different crystal structures (α′, β, γ, δ, ε, ζ) using various synthesis routes, as shown in eqn (2).

$$3LiH + AlCl_3 + nEt_2O \rightarrow AlH_3 \cdot nEt_2O + 3LiCl \quad (1)$$

$$3LiAlH_4 + AlCl_3 + Et_2O \rightarrow 4AlH_3 + 3LiCl\downarrow + Et_2O\uparrow \quad (2)$$

Nowadays AlH_3 is typically synthesized with organic methods. However, this route of synthesis has drawbacks in industrialization due to the high cost of the reagents and the complicated techniques dealing with AlH_3. Therefore, it is imperative to perform chemical conversion in a solvent-free condition for direct synthesis of non-solvated AlH_3.[15] One solvent-free mechanochemical method to synthesize AlH_3 was investigated by cryomilling $LiAlD_4$ and $AlCl_3$ at −196 °C.[16] Decomposition of AlH_3 can be remarkably reduced with this route. But the whole process of solid state reaction has to be kept at a very low temperature, which probably hinders the large-scale production of AlH_3. It was also demonstrated by Dinh that thermochemical transformation to AlH_3 is possible at a low temperature of 75 °C using $LiAlH_4$ and $AlCl_3$ as reagents,[17] as shown in eqn (3). Nevertheless, this thermochemical transformation needs continuous mixing in heating treat and may encounter some problems on formation of low melting eutectics.

$$3LiAlH_4 + AlCl_3 \rightarrow 4AlH_3 + 3LiCl \quad (3)$$

With the development of efficient and cost-effective mechanochemical methods to synthesize AlH_3,[15] the effects of fluoride as the catalyst during reactive ball milling were demonstrated.[18] It was later reported by Sartori that the relative content of α′ phase can increase to 1.05 by adding FeF_3 to the reagents.[19] Followed by the above reports, it was discovered that the crystal structure of additives could play an important role in synthesizing various alane polymorphs,[20] and additives with the same crystal structure of alane could lead to the formation of isostructural AlH_3 phase. Graham *et al.*[21] also proposed a method of synthesizing AlH_3–TEDA with Ti as the catalyst, which regenerated AlH_3 under lower hydrogen pressure. Moreover, it was confirmed by Sandrock that the addition of LiH has a destabilization effect on AlH_3 and can enhance H_2 desorption kinetics.[22]

Among the considerable additives, it was clarified by Hanada and Isobe[23,24] that 3d transition metals have excellent catalytic effects on hydrogen-storage materials such as Mg-based alloys, sodium alanate and so on. Moreover, recent studies show that

School of Materials Science and Engineering, Harbin Institute of Technology, Harbin, 150001, China. E-mail: hulx@hit.edu.cn; Tel: +86 0451 86418613

† Electronic supplementary information (ESI) available: Material preparation, hydrogen desorption measurements and reagent characterization. See DOI: 10.1039/c4ra16635c

the reaction kinetics of hydride can be effectively improved using transition metals as catalysts. Although Tsuda[25] demonstrated that the catalytic activities of element Zn is considerably low due to full occupancies of the 3d and 4s orbits, it was later described by Hu[26] that mixing with catalytic transition elements such as Zn and Zr could improve the hydriding kinetics of Mg efficiently at ambient temperature. Solid–gas reaction on the full hydrogenation of Mg–5.5% Zn–0.6% Zr (mass%) alloy was applied to accelerate the reaction. The average grain size of the MgH_2 phase obtained by milling can reach between 8 and 10 nm. Previously, we found that the solid state reaction milling is a cost-effective way to synthesize AlH_3 when reagents are chosen properly, and nano-sized AlH_3 can be successfully synthesized in a shorter time using cheaper nanocrystalline MgH_2 and $AlCl_3$ as reagents. As described in the present work, it is surprising to find that the reaction rate and the dehydrogenation of the product may be regulated in the presence of the 3d transition metals. Therefore, this preliminary finding presents a rare example of elements Zn and Zr on synthesis of the nano-sized AlH_3 phase as well as its de-hydriding properties.

All the steps were carried out inside a glove box filled with purified argon gas. The nanocrystalline MgH_2 (I) was formed by full hydrogenation of pure Mg powders, while MgH_2 (II) was formed by milling Mg–5.5% Zn–0.6% Zr (mass%) alloy in hydrogen (see Fig. S1 and S2, ESI†). $AlCl_3$ powders (3 : 2) were used as the starting reagents in both MgH_2 nanocrystallines without further purification. The MgH_2–$AlCl_3$ reaction is finished accompanied with the formation of γ-AlH_3 after milling for 25 h (refer to ESI†).

The hydrogen desorption was measured with a special home-made vacuum apparatus by volumetric method (refer to ESI†). The amounts of hydrogen were calculated by the ideal gas equation using the obtained data. Subsequently, the content of AlH_3 in its nanocomposite was obtained. Based on theoretical yield of mechanochemical reaction and above results, the de-hydriding kinetics curves of $AlH_3/MgCl_2$ nanocomposite are presented. Moreover, thermal analysis was performed on a differential scanning calorimeter (refer to ESI†).

In order to investigate the effects of Zn and Zr on the synthesis of the $AlH_3/MgCl_2$ composite, Fig. 1 shows the XRD patterns of both MgH_2 (I) and MgH_2 (II) with $AlCl_3$ powders by mechanical milling for 4, 16 and 25 h. As can be seen in Fig. 1a, the XRD pattern of the MgH_2–$AlCl_3$ mixture after milling for 4 h consisted of obvious peaks assigned to γ-AlH_3, indicating that elements Zn and Zr contained in MgH_2 (II) could accelerate the mechano-chemical reaction. Meanwhile, diffraction peaks of the MgH_2 phase can also be detected from Fig. 1a and it was attributed to the unfinished mechanochemical reaction between MgH_2 and $AlCl_3$. After milling for 16 h, the diffraction peaks of the MgH_2 phase disappeared, and MgH_2 in the powder was completely transformed into AlH_3 and $MgCl_2$ phases (see Fig. 1b). Therefore, XRD pattern results could be used as an indicator of termination of the reaction. In addition, the phenomenon that the peak for AlH_3 synthesized by MgH_2 (II) is wider than the diffraction peak without adding Zn and Zr. Even milling for 25 h, the diffraction peaks of the γ-AlH_3 phase produced by MgH_2 (II) was still wider than MgH_2 (I). This is

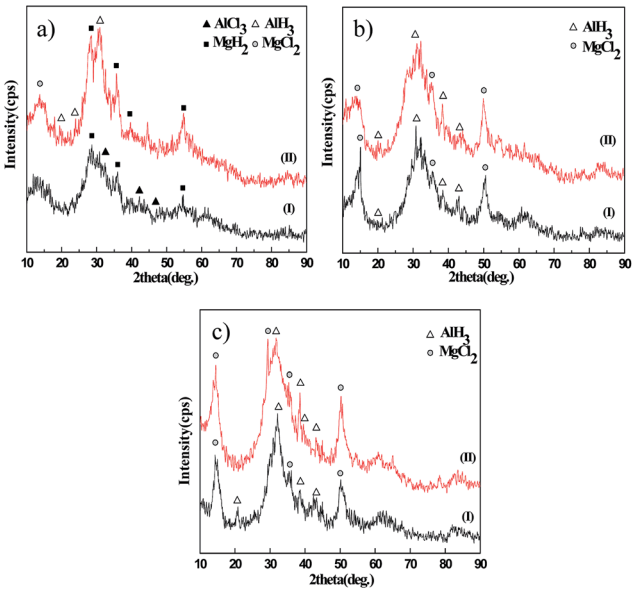

Fig. 1 XRD patterns from mechanochemical synthesized $AlH_3/MgCl_2$ composite milled by (I) and (II) with $AlCl_3$ for different time: (a) 4 h, (b) 16 h, (c) 25 h.

attributed to elements Zn and Zr contained in MgH_2 (II) which can form nano-sized γ-AlH_3 phase with much thinner crystallite size. Finally, compared with AlH_3 synthesized by MgH_2 (I), it was clarified that the average grain size of γ-AlH_3 produced by MgH_2 (II) milled for 25 h can reach 5.5 nm. From the above results, it is possible that the reaction rate and grain size of AlH_3 may be partially responsible for the catalytic mechanism, which needs future investigation.

Although AlH_3 is sensitive to high energy electron beam, Beattie revealed the TEM image and the selected area diffraction pattern (SADP) which obviously respond to the α phase.[27] Fig. 2 shows the AlH_3 nano-composite synthesized at room temperature which was still embedded with the $MgCl_2$. It can be seen from Fig. 2a that when the mixture was milled by MgH_2 (I) and $AlCl_3$ for 25 h, particles and spots can be observed from the bright field image and the corresponding electron diffraction (ED) pattern. It is evident that AlH_3 which was transformed into nanocrystalline at the ultimate milling stage and the nano-particles with whose size was around 12 nm were detected in the composite. The details of the crystal structure of the as-milled nano-particles was further studied by High Resolution Transmission Electron Microscopy (HRTEM), which characteristically suggests that the $AlH_3/MgCl_2$ nano-composite is consisted of fine crystallized particles with different crystal orientations. Besides, the lattice fringes observed in Fig. 2b correspond to (107), (113) and (214) planes with distances of 0.198, 0.173 and 0.115 nm respectively. The typical lattice spacing which is determined to be 0.152, 0.226 and 0.302 nm is attributed to the lattice distance of γ-AlH_3 phase. The TEM image shown in Fig. 2c is the composite milled by MgH_2 (II) and $AlCl_3$ for 25 h. Compared with the above results without Zn and Zr in the reagents, it is shown that the crystallite size of γ-AlH_3 was approximately 5.5 nm on average, which is in accordance

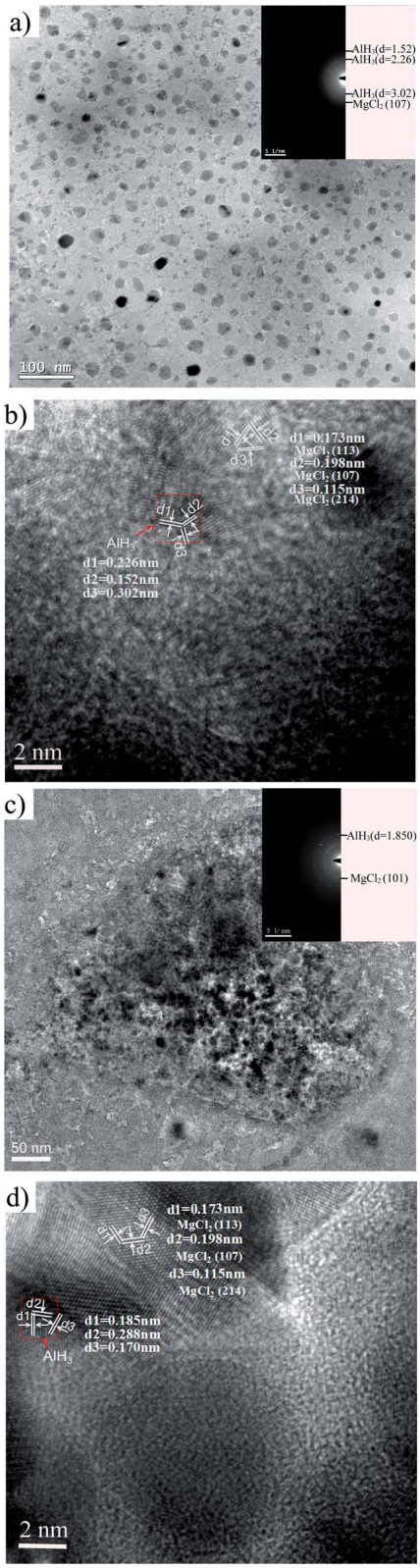

Fig. 2 TEM images as well as electron diffraction patterns and corresponding HRTEM photos of $AlH_3/MgCl_2$ nanocomposite milling for 25 h: (a) and (b) were obtained by milling (I) and $AlCl_3$. (c) and (d) were gained by synthesizing (II) and $AlCl_3$.

with the XRD results. The ED pattern (inset of Fig. 3c) of the selected region suggests that this nanocomposite is crystalline containing (101) plane of the $MgCl_2$ and AlH_3 crystal lattice. Moreover, the parallel lattice fringes shown in Fig. 2d further identified that the product has a perfect match with the γ phase in the miller index (the distance of 0.288, 0.185, 0.170 nm between planes results from the lattice spacing of the γ phase).

The dehydriding properties of the $AlH_3/MgCl_2$ nanocomposite were studied under isothermal processes between 150 and 220 °C. It can be seen from Fig. 3 that the curves exhibit similarly with other materials in decomposition with an accelerating stage followed by decaying stages. Fig. 3a shows the hydrogen desorption curves of the composite synthesized by MgH_2 (I) and (II) heated at 150 °C. It is found that dehydriding process did not terminate at 2×10^4 s. Besides, the as-milled γ-phase existing in the composite presents relatively undesirable dynamic properties. According to the report by Graetz that full dehydrogenation of γ-AlH_3 can be achieved at 138 °C within 6×10^3 s, resulting from the mechanism that the solid-state decomposition is primarily affected by the nucleation and growth of Al in two and three dimensions.[28] While in this study, it is attributed to the obtained $AlH_3/MgCl_2$ composite consisted of a large amount of $MgCl_2$ as a byproduct which hindered the growth of the Al phase in progress of the decomposition. With the dehydriding temperature increasing from 150 to 220 °C, the time of full decomposition decreased rapidly. Compared with the $AlH_3/MgCl_2$ composite produced by MgH_2 (I) without adding Zn and Zr, AlH_3 has a perfect dehydriding property with a 9.69 wt% of hydrogen content at 205 °C for 8×10^3 s (see Fig. 3c). When the temperature increased to 220 °C for approximately 2.2×10^3 s, it is also identified that the dehydriding rate of nano-sized AlH_3 was faster than the product

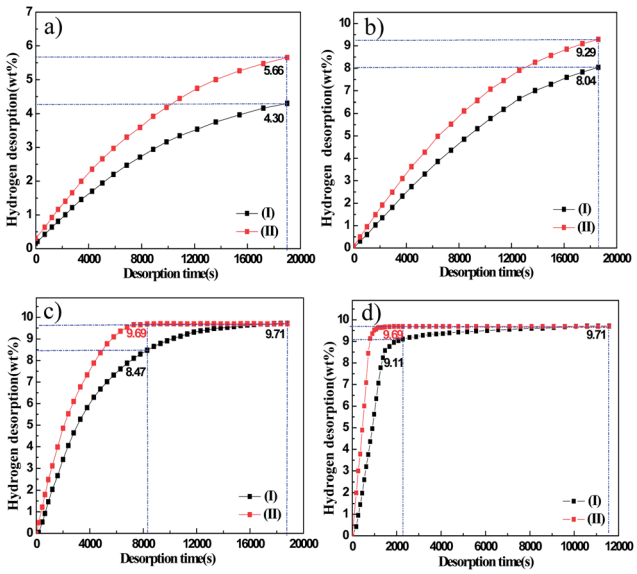

Fig. 3 The de-hydriding kinetics curves of $AlH_3/MgCl_2$ nanocomposite synthesized by (I) and (II) with various temperatures: (a) 150 °C, (b) 170 °C, (c) 205 °C, (d) 220 °C.

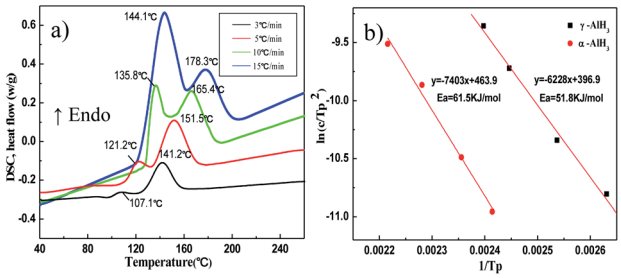

Fig. 4 (a) DSC curves of $AlH_3/MgCl_2$ nanocomposite synthesized by MgH_2 (II) in temperature ranges from 40 to 260 °C; (b) the apparent energy for the decomposition obtained from DSC measurements.

heated at 205 °C, and AlH_3 added with Zn and Zr has a more desirable dehydriding dynamics. Consequently, the elements Zn and Zr probably come into play with the decomposition kinetics of AlH_3 and can accelerate the dehydriding reaction of AlH_3. The results have good correspondence with the report addressed by Graetz who also found that decomposition kinetics of AlH_3 can be accelerated with the diffusion effect of the Ti doping.[29]

In order to gain a deep insight into the effects of Zn and Zr addition on the desorption property, the dehydriding kinetics of $AlH_3/MgCl_2$ composite synthesized by MgH_2 (II) were further investigated by Kissinger's method, and the apparent activation energy (E_a) was formulated by eqn (4).

$$\ln \frac{c}{T_p^2} = -\frac{E_a}{RT_p} + A \quad (4)$$

where c is the heating rate during the DSC process, T_p is the absolute temperature corresponding to the maximum desorption rate, which can be obtained from the measured DSC curves. R is the universal gas constant with a value of 8.314 J mol^{-1} K^{-1}, and A is a constant. Fig. 4a shows the DSC plots of $AlH_3/MgCl_2$ composite synthesized by MgH_2 (II) at various heating rates. An exothermic peak and two endothermic peaks are observed at the temperature range of 94–98 °C, 105–110 °C and 120–160 °C, respectively. It is clear that three reactions including the transition and decomposition of γ-AlH_3 as well as the decomposition of α phase occurred in the whole heating process, and this result has a similarity on the report addressed by Graetz.[30] It was illustrated by Ouyang *et al.* that the dehydriding process can be catalyzed by the combination of $CeH_{2.73}$ and Ni to MgH_2.[31] Also, Liu verified that NbF_5 addition dramatically reduced the activation energy and improved the hydrogen desorption kinetics of the MgH_2–AlH_3 composite.[32] According to the DSC outcomes, the apparent activation energy for the dehydriding reaction is calculated based on the slope measurement (see Fig. 4b). For the decomposition of γ phase, E_a is estimated to be 51.8 KJ mol^{-1}. As expected, this value is lower than MgH_2–AlH_3 composite (77.6 KJ mol^{-1}).[33] Additionally, it is discovered that the activation energy of α-AlH_3 which transformed from the γ phase changed remarkably compared to that of the pure phase. All the above phenomena are attributed to the effects of Zn and Zr addition on the AlH_3 composite.

Conclusions

The effect of elements Zn and Zr on synthesis of $AlH_3/MgCl_2$ nano-composite and its dehydrogenation behaviour were reported as a rare example in this paper. Firstly, addition of elements Zn and Zr could accelerate the process of mechanically-activated solid state reaction. Secondly, when milling for the same time, the average grain size of γ-AlH_3 doped with Zn and Zr was much finer which can reach 5.5 nm. The de-hydriding rate of nanosized AlH_3 which was synthesized by MgH_2 (II) was faster than un-doped AlH_3. The apparent energy for the hydrogen desorption of γ-AlH_3 in its composite was estimated to be 51.8 KJ mol^{-1}, which is much lower than undoped γ phase. If the temperature increased to 220 °C, the hydrogen desorption of AlH_3 can reach 9.69 wt% which impelled AlH_3 as a promising hydrogen storage material.

It should be noted that although $AlH_3/MgCl_2$ nano-composite is synthesized in this study, extraction process to get pure AlH_3 is needed before it can be applied as a hydrogen storage candidates. Presently, the most popular method for extracting AlH_3 is to generate etherate first and then extract AlH_3 by subsequent thermal cleavage. However, this method is complicated and not economical because of a large mount of ether is needed to wash the $LiAlH_4$.[34] Similarly, Paskevicius *et al.* achieved great success in extracting AlH_3 from LiCl by washing it with nitromethane.[16] However, satisfactory results could not be obtained with this method in our extracting process, because the by-product ($MgCl_2$) can not be dissolved in nitromethane. Although AlH_3 is very reactive with many solvent due to its reducibility, the extraction can still be performed when an appropriate solvent is selected. The extraction process will be studied and discussed in details in the future.

Notes and references

1 G. Frenette and D. Forthoffer, *Int. J. Hydrogen Energy*, 2009, **34**, 3578–3588.
2 H. J. Neef, *Energy*, 2009, **34**, 327–333.
3 M. Contestabile, G. J. Offer, R. Slade, F. Jaeger and M. Thoennes, *Energy Environ. Sci.*, 2011, **4**, 3754–3772.
4 P. Corbo, F. Migliardini and O. Veneri, *Renewable Energy*, 2009, **34**, 1955–1961.
5 D. Mori and K. Hirose, *Int. J. Hydrogen Energy*, 2009, **34**, 4569–4574.
6 L. Schlapbach and A. Züttel, *Nature*, 2001, **414**, 353–358.
7 M. Felderhoff, C. Weidenthaler, R. von Helmolt and U. Eberle, *Phys. Chem. Chem. Phys.*, 2007, **9**, 2643–2653.
8 N. L. Rosi, J. Eckert, M. Eddaoudi, D. T. Vodak, J. Kim, M. O'Keeffe and O. M. Yaghi, *Science*, 2003, **300**, 1127–1129.
9 Y. Liu, J. F. Eubank, A. J. Cairns, J. Eckert, V. C. Kravtsov, R. Luebke and M. Eddaoudi, *Angew. Chem., Int. Ed.*, 2007, **46**, 3278–3283.
10 J. R. Li, Y. Tao, Q. Yu, X. H. Bu, H. Sakamoto and S. Kitagawa, *Chem.–Eur. J.*, 2008, **14**, 2771–2776.
11 J. Graetz, J. J. Reilly, V. A. Yartys, J. P. Maehlen, B. M. Bulychev, V. E. Antonov, B. P. Tarasov and I. E. Gabis, *J. Alloys Compd.*, 2011, **509**, S517–S528.

12 H. Saitoh, A. Machida, Y. Katayama and K. Aoki, *Appl. Phys. Lett.*, 2008, **93**, 151918.
13 A. E. Finholt Jr, A. C. Bond and H. I. Schlesinger, *J. Am. Chem. Soc.*, 1947, **69**, 1199–1203.
14 F. M. Brower, N. E. Matzek, P. F. Reigler, H. W. Rinn, C. B. Roberts, D. L. Schmidt and K. Terada, *J. Am. Chem. Soc.*, 1976, **98**, 2450–2453.
15 S. Gupta, T. Kobayashi, I. Z. Hlova, J. F. Goldston, M. Pruski and V. K. Pecharsky, *Green Chem.*, 2014, **16**, 4378–4388.
16 M. Paskevicius, D. A. Sheppard and C. E. Buckley, *J. Alloys Compd.*, 2009, **487**, 370–376.
17 L. V. Dinh, D. A. Knight, M. Paskevicius, C. E. Buckley and R. Zidan, *Appl. Phys. A: Mater. Sci. Process.*, 2012, **107**, 173–181.
18 H. W. Brinks, A. Istad-Lem and B. C. Hauback, *J. Phys. Chem. B*, 2006, **110**, 25833–25837.
19 S. Sartori, A. Istad-Lem, H. W. Brinks and B. C. Hauback, *Int. J. Hydrogen Energy*, 2009, **34**, 6350–6356.
20 J. E. Fonneløp, S. Sartori, M. H. Sørby and B. C. Hauback, *J. Alloys Compd.*, 2012, **540**, 241–247.
21 D. D. Graham, J. Graetz, J. Reilly, J. E. Wegrzyn and I. M. Robertson, *J. Phys. Chem. C*, 2010, **114**, 15207–15211.
22 G. Sandrock, J. Reilly, J. Graetz, W. M. Zhou, J. Johnson and J. Wegrzyn, *Appl. Phys. A: Mater. Sci. Process.*, 2005, **80**, 687–690.
23 N. Hanada, T. Ichikawa and H. Fujii, *J. Phys. Chem. B*, 2005, **109**, 7188–7194.
24 S. Isobe, T. Ichikawa, J. I. Gottwald, E. Gomibuchi and H. Fujii, *J. Phys. Chem. Solids*, 2004, **65**, 535–539.
25 M. Tsuda, W. A. Diño, H. Kasai, H. Nakanishi and H. Aikawa, *Thin Solid Films*, 2006, **509**, 157–159.
26 L. Hu, H. Wang and X. Wang, *J. Alloys Compd.*, 2012, **513**, 343–346.
27 S. D. Beattie, T. Humphries, L. Weaver and G. S. McGrady, *Chem. Commun.*, 2008, **37**, 4448–4450.
28 J. Graetz and J. J. Reilly, *J. Phys. Chem. B*, 2005, **109**, 22181–22185.
29 J. Graetz, J. J. Reilly, J. G. Kulleck and R. C. Bowman, *J. Alloys Compd.*, 2007, **446**, 271–275.
30 J. Graetz and J. J. Reilly, *J. Alloys Compd.*, 2006, **424**, 262–265.
31 L. Z. Ouyang, X. S. Yang, M. Zhu, J. W. Liu, H. W. Dong, D. L. Sun, J. Zou and X. D. Yao, *J. Phys. Chem. C*, 2014, **118**, 7808–7820.
32 H. Liu, X. Wang, Y. Liu, Z. Dong, S. Li, H. Ge and M. Yan, *J. Phys. Chem. C*, 2014, **118**, 18908–18916.
33 H. Liu, X. Wang, Y. Liu, Z. Dong, H. Ge, S. Li and M. Yan, *J. Phys. Chem. C*, 2013, **118**, 37–45.
34 B. M. Bulychev, V. N. Verbetskii, A. I. Sizov, T. M. Zvukova, V. K. Genchel' and V. N. Fokinl, *Russ. Chem. Bull.*, 2007, **56**, 1305–1312.

